Radial magnetic field in magnetic confinement device*

Xiong Hao(熊 昊)[a)b)], Liu Ming-Hai(刘明海)[a)b)†], Chen Ming(陈 明)[a)b)], Rao Bo(饶 波)[a)b)], Chen Jie(陈 杰)[a)b)], Chen Zhao-Quan(陈兆权)[c)], Xiao Jin-Shui(肖金水)[a)b)], and Hu Xi-Wei(胡希伟)[a)b)]

[a)] State Key Laboratory of Advanced Electromagnetic Engineering and Technology, Huazhong University of Science and Technology, Wuhan 430074, China
[b)] School of Electrical and Electric Engineering, Huazhong University of Science and Technology, Wuhan 430074, China
[c)] College of Electrical and Information Engineering, Anhui University of Science and Technology, Huainan 232001, China

(Received 29 December 2014; revised manuscript received 9 April 2015; published online 20 July 2015)

The intrinsic radial magnetic field (B_r) in a tokamak is explored by the solution of the Grad–Shafranov equation in axisymmetric configurations through an expansion of the four terms of the magnetic surfaces. It can be inferred from the simulation results that at the core of the device, the tokamak should possess a three-dimensional magnetic field configuration, which could be reduced to a two-dimensional one when the radial position is greater than $0.6a$. The radial magnetic field and the amzimuthal magnetic field have the same order of magnitude at the core of the device. These results can offer a reference for the analysis of the plasma instability, the property of the core plasma, and the magnetic field measurement.

Keywords: radial magnetic field, minor toroidal coordinate, three-dimensional magnetic field configuration

PACS: 52.55.–s, 52.55.Fa, 52.55.Dy **DOI:** 10.1088/1674-1056/24/9/095202

1. Introduction

Tokamak-type devices are one of several types of magnetic confinement devices, and are one of the most promising candidates for producing controlled thermonuclear fusion. The total magnetic field in a tokamak is complex and of a helical shape, which is generated by the various coils' currents and the electric current that flows inside the plasma. The toroial magnetic field is easily obtained in the coordinate system (R, φ, Z) as

$$B_\varphi = \frac{\mu I}{2\pi R},$$

the poloidal magnetic field is about 10^{-3}–$10^{-2}B_\varphi$, and the radial magnetic field B_r is commonly known as the error field which is generally considered to be majorly generated by the coil misalignments and the non-axisymmetric current. The radial magnetic field is relatively significantly smaller than the poloidal magnetic field, which can be neglected in most cases. However it plays a crucial role in instability analyses.

Rogers and his colleagues illustrated the importance of the radial magnetic field in the fast reconnection in a collisionless system depending on the dynamics of whistler and/or kinetic Alfvén waves at small scales, where no quadratic waves can exist and the reconnection rate is very small when $B_r^2 \ll B_t^2 m_e/m_i$, $\beta \ll m_e/m_i$.[1] Buratti and Giovannozzi also proved that several Gs of B_r at the X point induces a fast magnetic reconnection and sawtooth collapses.[2,3] The low-m tearing modes, which often reduce the constraint ability of the devices, can even stop rotation due to the locking effect of the vacuum vessel and the error field.[4–6] This effect is called mode penetration or error field penetration. The experimental results showed that the penetration threshold of an error field is very small; for J-TEXT with a current of 180 kA, the amplitude of the 2/1 component of the error field at the plasma edge is measured to be 0.31 G, which is about 1.8×10^{-5} B_t.[7,8] Up to now, many studies have focused on the physical models of the mode penetrations.[9–15]

All of these viewpoints indicate that a very small B_r is of great significance to the magnetic reconnection and the tearing mode in a tokamak. In the past, scholars used to think that the radial magnetic field B_r was the error field generated by the coils' misalignments and the non-axisymmetric current feeds. However, when calculating the magnetic field in the minor toroidal coordinate system (r, θ, φ), it turns out that the intensity of the intrinsic radial magnetic field is equivalent to the azimuthal magnetic field at the core of the plasma ($r < 0.2a$). Therefore, in this paper, the Grad–Shafranov equation is solved in the minor toroidal coordinate system, the results of numerical simulations show that there is a three-dimensional magnetic field structure at the core, and the radial magnetic field in the tokamak is considered to be produced by a combination of the intrinsic radial field and the error field.

The aim of this work is to calculate the magnetic field configuration in the minor toroidal coordinate system (r, θ, φ), especially the intrinsic quantity of the radial magnetic field at the core of the plasma. As a result, it can offer a reference for the analysis of the plasma instability, the property of the core plasma, and the magnetic field measurement. The article is organized as follows. The physical model is presented in Section 2, followed by the simulation results in Section 3. The discussion and conclusion are presented in Section 4.

*Project supported by the Special Domestic Program of ITER, China (Grant No. 2009GB105003).
†Corresponding author. E-mail: mhliu@hust.edu.cn
© 2015 Chinese Physical Society and IOP Publishing Ltd

2. Physical model

2.1. The plasma equilibrium

We solve the Grad–Shafranov equation in the minor toroidal coordinate system (r, θ, φ), where r is the minor radial coordinate, φ is the toroidal angle, and θ is the azimuthal angle in the clockwise direction. Under the axisymmetrical hypothesis, the magnetic field is supposed to be independent of the toroidal angle φ.

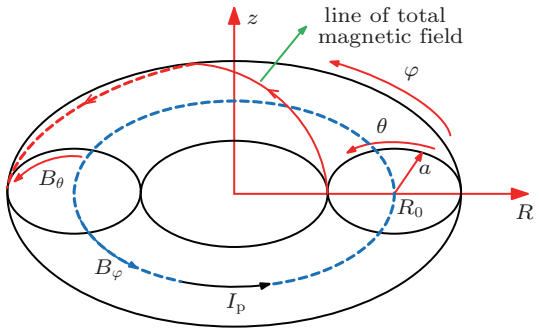


Fig. 1. (color online) The minor toroidal coordinate system.

Figure 1 is a diagram of the minor toroidal coordinate system. The quantitative relation between the minor toroidal coordinate system (r, θ, φ) and the major toroidal coordinate system (R, φ, Z) is

$$r\cos\theta = R - R_0, \quad r\sin\theta = -Z.$$

The following is obtained through the Ampere law:

$$\frac{1}{r}\frac{\partial B_\varphi}{\partial\theta} - \frac{B_\varphi}{R}\sin\theta = \mu_0 j_r, \tag{1}$$

$$\frac{B_\varphi}{R}\cos\theta + \frac{\partial B_\varphi}{\partial r} = -\mu_0 j_\theta, \tag{2}$$

$$\frac{1}{r}\left(\frac{\partial(rB_\theta)}{\partial r} - \frac{\partial B_r}{\partial\theta}\right) = \mu_0 j_\varphi. \tag{3}$$

Equation (3) is the Grad–Shafranov equation in the minor toroidal coordinate system[16]

$$j_\varphi = -\frac{1}{2\pi R\mu_0}\left[\Delta_0\psi - \frac{1}{R}\left(\cos\theta\frac{\partial}{\partial r} - \frac{\sin\theta}{r}\frac{\partial}{\partial\theta}\right)\psi\right]. \tag{4}$$

From Eqs. (1) and (2), the toroidal magnetic field should be revised when the angular current is considered.

The two-fluid modes regardless of impurity are

$$nm_\mathrm{i}\frac{\mathrm{d}\boldsymbol{u_i}}{\mathrm{d}t} + \nabla p_\mathrm{i} = en\boldsymbol{E} + en(\boldsymbol{u_i}\times\boldsymbol{B}) + \frac{m_\mathrm{e}n}{\tau_\mathrm{ei}}(\boldsymbol{u_e} - \boldsymbol{u_i}), \tag{5}$$

$$nm_\mathrm{e}\frac{\mathrm{d}\boldsymbol{u}_\mathrm{e}}{\mathrm{d}t} + \nabla p_\mathrm{e} = -en\boldsymbol{E} - en(\boldsymbol{u}_\mathrm{e}\times\boldsymbol{B}) - \frac{m_\mathrm{e}n}{\tau_\mathrm{ei}}(\boldsymbol{u_e} - \boldsymbol{u_i}), \tag{6}$$

where m_i and m_e are the masses of the ions and the electrons, respectively, $\boldsymbol{u}_\mathrm{i}$ and $\boldsymbol{u}_\mathrm{e}$ are their speeds; $p_\mathrm{i} = nT_\mathrm{i}$ and $p_\mathrm{e} = nT_\mathrm{e}$ are their pressures; T_i and T_e are their temperatures; and τ_ei is the collision time of ions and electrons.

The following is obtained by adding Eqs. (5) and (6) ($nm_\mathrm{i} + nm_\mathrm{e} \approx nm_\mathrm{i}$, the electron's inertia is neglected):

$$m_\mathrm{i}n\frac{\mathrm{d}\boldsymbol{u}_\mathrm{i}}{\mathrm{d}t} + \nabla p = \boldsymbol{j}\times\boldsymbol{B},$$

where $p = p_\mathrm{i} + p_\mathrm{e}$ is the total pressure, and $\boldsymbol{j} = en(\boldsymbol{u}_\mathrm{i} - \boldsymbol{u}_\mathrm{e})$ is the total current density.

The equilibrium equation in a steady state of no flow is

$$\nabla p = \boldsymbol{j}\times\boldsymbol{B}. \tag{7}$$

It can be seen that the three have similar shape distributions spatially.

The relations among the magnetic field, the magnetic surface, and the poloidal current I are defined as

$$B_\theta = -\frac{1}{2\pi R}\frac{\partial\psi}{\partial r}, \tag{8}$$

$$B_r = \frac{1}{2\pi Rr}\frac{\partial\psi}{\partial\theta}, \tag{9}$$

$$j_\theta = -\frac{1}{2\pi R}\frac{\partial I}{\partial r}, \tag{10}$$

$$j_r = \frac{1}{2\pi Rr}\frac{\partial I}{\partial\theta}. \tag{11}$$

The following is obtained by substituting Eqs. (8) and (10) to the radial component of Eq. (7):[17]

$$\frac{\partial p}{\partial r} = \frac{1}{2\pi R}\left(j_\varphi\frac{\partial\psi}{\partial r} - B_\varphi\frac{\partial I}{\partial r}\right). \tag{12}$$

From the above formula, we can obtain

$$j_\varphi = (2\pi Rp_\mathrm{s} + I_{\theta\mathrm{s}}B_\varphi)/\psi_\mathrm{s}. \tag{13}$$

The following is obtained by substituting Eq. (13) to Eq. (4):

$$\Delta^*\psi = -2\pi\mu_0(2\pi R^2p_\mathrm{s} + I_\mathrm{s}B_\mathrm{t}R_0)\psi_\mathrm{s}. \tag{14}$$

The magnetic surfaces are expanded to the 4th-order terms. Therefore, the initial value of the magnetic surface can be set as

$$\begin{aligned}\psi(0,\theta) \;=\; & a_0(0) + a_1(0)\cos\theta + a_2(0)\cos2\theta \\ & + a_3(0)\cos3\theta,\end{aligned} \tag{15}$$

where a_0, a_1, a_2, a_3 are the adjusting coefficients of the initial value of the magnetic surface.

The spatial distribution equations of pressure and current can be set as

$$\begin{aligned}p &= p_0 + A_1\psi + A_2\psi^2, \\ I &= I_0 + B_1\psi + B_2\psi^2,\end{aligned} \tag{16}$$

where p_0, A_1, A_2, I_0, B_1, B_2 are the corresponding coefficients of pressure and current, respectively.

The central difference scheme is used for iteration for Eq. (4). For any point (r_i, θ_j),

$$r_\mathrm{i} = (i + 0.5)\Delta r, \quad i = 0, 1, 2, \ldots,$$

$$\theta_j = j\Delta\theta, \quad j = 0, 1, 2, \ldots$$

The spatial step is 0.01 m, and the angle can be equally divided into 26 parts.

The boundary condition is eliminating the singularity around $r = 0$,

$$\lim_{r\to 0^+} r\frac{\partial \psi}{\partial r} = 0. \tag{17}$$

The boundary value can be obtained from Eq. (17) after the initial value of the magnetic surface is set. Through iteration by using the difference scheme of Eq. (14), the whole balancing magnetic surface distribution is obtained after some adjustments of a_0, a_1, a_2, a_3.

2.2. Magnetic field in (r, θ, φ)

The magnetic field configuration is important for the takamak plasma. In the past, the magnetic surface of the tokamak plasma was solved in the magnetic surface coordinate (ψ, θ, φ). Since the magnetic flux along the magnetic surface is irrelevant to the poloidal angle of the magnetic surface coordinate, the magnetic field in the magnetic surface coordinate system is equal to the two-dimensional spiral magnetic field, including only the poloidal magnetic field and the toroidal magnetic field. The position of every magnetic surface is difficult to identify and the shafranov displacement of every magnetic surface is not equal in the experiment. Therefore, when comparing the magnetic field data obtained in the magnetic surface coordinate and the experimental data, special attention should be paid to the difference between the position in the magnetic surface coordinate and the position in the spatial coordinate with the original point set at the device center.

However, in the minor toroidal coordinate system, the magnetic flux is a function concerning radius r and azimuthal angle θ,

$$\psi(r, \theta) = a_0(r) + a_1(r)\cos\theta + a_2(r)\cos 2\theta + a_3(r)\cos 3\theta.$$

The three-dimensional magnetic field results can be obtained when solving the magnetic field of the tokamak plasma in the minor toroidal coordinate system, which includes the toroidal magnetic field, the azimuthal magnetic field, and the radial magnetic field (the radial direction centers at the original point of the minor radius coordinate system),

$$\begin{aligned} B_\theta &= -\frac{1}{2\pi R}\frac{\partial \psi}{\partial r} \\ &= -\frac{1}{2\pi R}\left(\frac{\partial a_0}{\partial r} + \frac{\partial a_1}{\partial r}\cos\theta + \frac{\partial a_2}{\partial r}\cos 2\theta + \frac{\partial a_3}{\partial r}\cos 3\theta\right) \\ &= B_\theta^0 + B_\theta^1\cos\theta + B_\theta^2\cos 2\theta + \cdots, \\ B_r &= \frac{1}{2\pi R r}\frac{\partial \psi}{\partial \theta} \\ &= \frac{1}{2\pi R r}(-a_1\sin\theta - 2a_2\sin 2\theta - 3a_3\sin 3\theta) \\ &= B_r^1\sin\theta + B_r^2\sin 2\theta + \cdots. \end{aligned}$$

From the above, the source of the intrinsic radial magnetic field can be seen clearly.

3. Results of numerical simulations

In this paper, the azimuthal magnetic field is generated by the plasma current itself, thus the magnetic surface is also known as the net magnetic field. Shot number #1026968 of J-TEXT serves as the calculation basis, and the major and minor radii of the device are 1.05 m and 0.27 m, respectively, the device belongs to a middle-sized circular section of the tokamak (formerly TEXT in Texas of the United States and was rebuilt by Huazhong University of Science and Technology in 2006).[18] The discharge parameters of the plasma are as follows: $B_t = 1.60$ T, $I_p = 160$ kA, $n_{e0} \cong 3.225 \times 10^{19}$ m^{-3}, $T_{e0} \cong 0.9$ keV, $T_{i0} \cong 0.475$ keV.

3.1. Magnetic surfaces

Figure 2 depicts the contours of the magnetic surfaces in the (R, Z) plane. The maximum of the Shafranov shift (shift of the magnetic axis) is 2.148 cm, which occurs at the innermost magnetic surface. This is the displacement of the magnetic axis. While the Shafranov shift of the outmost magnetic surface is almost zero, which means that the outmost magnetic field is in good agreement with the device.

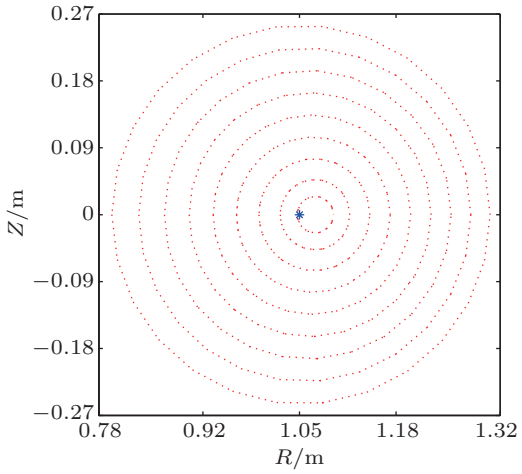


Fig. 2. (color online) Contours of magnetic surfaces.

3.2. The radius of magnetic surface and Shafranov shift

Figure 3 depicts the Shafranov shift with different radius of the magnetic surface. The Shafranov shift is inversely proportional to the radius of the magnetic surface. The discrepancies between r_s and r are especially cautious for the theoretical analysis, they are strictly equivalent only at the outermost position. Since the Shafranov shift at the core is large while the radius of the magnetic surface is small, the minor toroidal coordinate system reflects the furthest departure from

the magnetic surface coordinate system in the center of the device. However, at the outermost part of the device, the minor toroidal coordinate system basically coincides with the magnetic surface coordinate system, mainly because the center of every magnetic surface is constantly changing. As the minor toroidal coordinate system deviates a lot from the magnetic surface coordinate system at the core, the specific magnetic surface structure is unknown during the process of experimental measurements and in fact the azimuthal magnetic field instead of the poloidal magnetic field is measured. Therefore, the three-dimensional magnetic field structure can provide a significant reference to the experimental magnetic measurement.

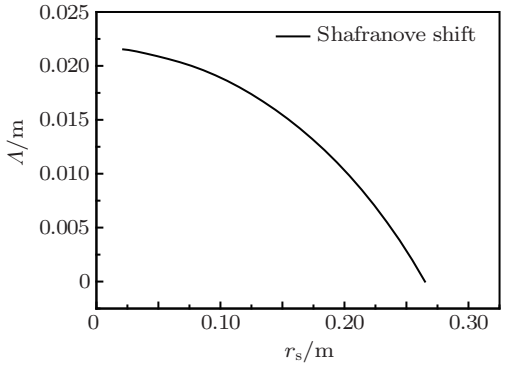


Fig. 3. Shafranov shift with different radius of the magnetic surface.

3.3. Perpendicular components of the magnetic field

In order to obtain a more accurate magnetic surface structure, the magnetic surface should be expanded to a higher order. In this way, the intrinsic radial magnetic field B_r could be obtained. The perpendicular magnetic field is defined as $B_\perp = \sqrt{B_r^2 + B_\theta^2}$. Figure 4 depicts the perpendicular components of the magnetic field. It can be easily seen that at the outermost part, the magnetic field is along the azimuthal direction of the minor toroidal coordinate system, while it shows a radial component at the core ($r < 0.2a$). The radial component of the magnetic field here means the intrinsic radial magnetic field. Meanwhile the data show that the first-order quantities (B_r^1, B_θ^1) of the radial magnetic field and the amzimuthal magnetic field remain at the same level everywhere. Particularly at the core ($r < 0.2a$), the first-order quantities (B_r^1, B_θ^1) of the radial magnetic field and the amzimuthal magnetic field are equivalent to the zero-order quantity (B_θ^0) of the amzimuthal magnetic field. Hence at the core, the radial magnetic field and the amzimuthal magnetic field have the same order of magnitude, which indicates that there exists an intrinsic three-dimensional magnetic field structure at the core ($r < 0.2a$). With the increase of the radius, the radial magnetic field is decreasing while the amzimuthal magnetic field is increasing, especially at $r > 0.6a$, the radial magnetic field is much smaller than the angular magnetic field. The magnetic field structure in the area of $r > 0.6a$ is two-dimensional, though there exists a significantly small fluctuating radial magnetic field B_r. The values of $B_\theta(a)$ and safety factor $q(a)$ at the edge of the plasma are 0.1185 T and 3.47, respectively, which are in good agreement with the experimental data. The above mentioned results fit well with the general properties of the magnetic flux in the frame of ideal MHD.[19,20]

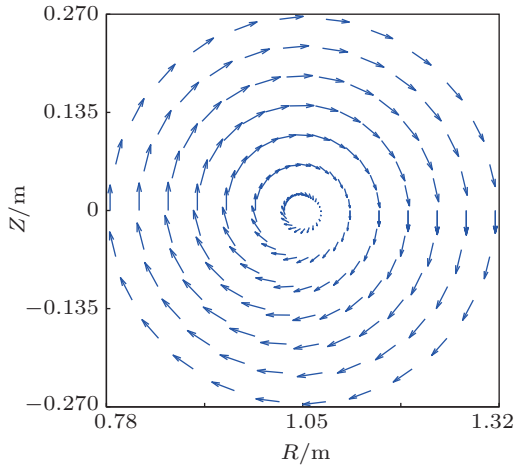


Fig. 4. (color online) The vector graph of $B_\perp$.

3.4. Magnetic field in the magnetic surface coordinate system

The radial magnetic field and the azimuthal magnetic field can be transferred to the poloidal magnetic field (B_p) and the magnetic field (B_r^s) perpendicular to the magnetic surface.

As shown in Fig. 5, the red circle is the magnetic surface at the core, and the dashed circle has its center at the geometric center and a radius of the radius of the magnetic surface.

The relationship between B_r, B_θ and B_r^s, B_p can be deduced as[21]

$$B_r^s = B_r \cos(\theta_s - \theta_c) + B_\theta \sin(\theta_s - \theta_c), \tag{18a}$$

$$B_p = -B_r \sin(\theta_s - \theta_c) + B_\theta \cos(\theta_s - \theta_c). \tag{18b}$$

Thus the magnetic field structure can be obtained in the magnetic surface coordinate system. The magnetic field (B_r^s) perpendicular to the magnetic surface is very small compared to the poloidal magnetic field and therefore can be neglected.

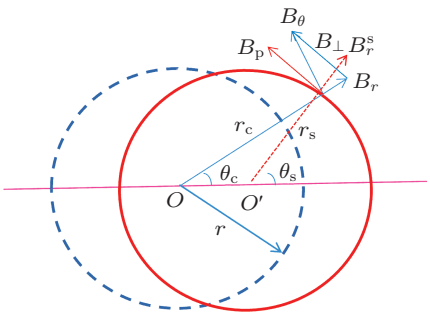


Fig. 5. (color online) Magnetic surface coordinate and minor toroidal coordinate.

Through Eq. (18), the poloidal magnetic field and the magnetic field perpendicular to the magnetic surface in the magnetic surface coordinate system can be obtained based on the radial magnetic field and the azimuthal magnetic field in the minor toroidal coordinate system. Figure 6 depicts the relationship between the poloidal magnetic field and the radius of the magnetic surface. At the core, the poloidal magnetic field is significantly small. However, it increases rapidly with the increase of the radius of the magnetic surface and reaches its maximum value 0.135 T when the radius of the magnetic surface increases to 0.2 m ($0.76a$), and then slightly decreases with the increase of the radius. The variation range of the poloidal magnetic field is probably between 0.02 T and 0.135 T. The intensity of the magnetic field perpendicular to the magnetic surface is about 10^{-4}–10^{-2} of the poloidal magnetic field, therefore, it can be neglected compared to the poloidal magnetic field. That is to say, the magnetic field perpendicular to the magnetic surface is almost zero and the perpendicular magnetic field $B_\perp$ is exactly the poloidal magnetic field. In the magnetic surface coordinate system, the magnetic field can be identified to have a two-dimensional structure. The results are identical to the magnetic field structure previously obtained in the magnetic surface coordinate system.

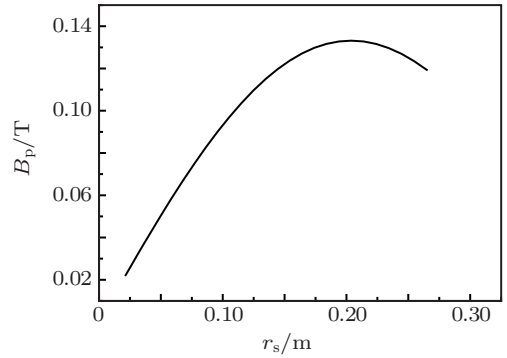


Fig. 6. Relation between the poloidal magnetic field and the raidus of the magnetic surface.

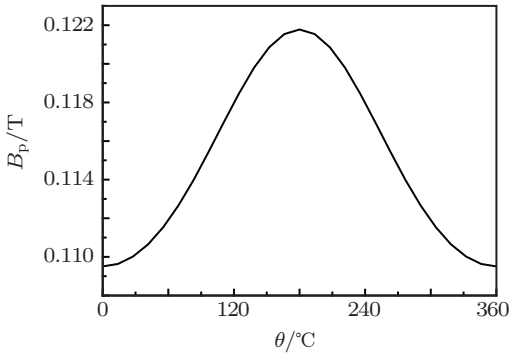


Fig. 7. Relation between the poloidal magnetic field and the poloidal angle ($r_s = 0.5a$).

Figure 7 is the changing law of the poloidal magnetic field with the change of the magnetic surface radius, where r_s is $0.5a$. From the above discussion, it is evident that the poloidal magnetic field at the strong field side is slightly larger than the poloidal magnetic field at the feeble field side, which is due to the toroidal effect.

4. Discussion and conclusion

The Grad–Shafranov equation is solved in the minor radius coordinate system by an expansion of the four terms of the magnetic surface. In the past, the intrinsic radial magnetic field was often neglected, which was considered as the error field. However, in this paper, the intrinsic radial magnetic field is obtained by solving the Grad–Shafranov equation in the minor toroidal coordinate system. That is to say, the radial magnetic field in a tokamak is considered to be produced by a combination of the intrinsic radial field and the error field. The existence of the intrinsic B_r has the following efficacies. 1) It can offer a reference for the analysis of the plasma instability such as sawtooths, tearing mode, etc. and the feature of the core plasma. 2) The first-order quantity of the magnetic field (B_r^1) is almost equivalent to the zero-order one (B_θ^0) at the core plasma, only a three-dimensional magnetic field structure is the real essence of the tokamak plasma. In this way, any charged particles can be frozen in the line of the magnetic field for an ideal MHD mode. Namely, the radial flow of plasma is doomed to happen because of the presence of the intrinsic radial magnetic B_r. For better understanding the plasma transport at the core, this property is of great importance. 3) Since the spatial coordinate relevant to the device is commonly used during the measurement process, the three-dimensional magnetic field solved in the minor toroidal coordinate system has more implications than the two-dimensional magnetic field. Therefore, the three-dimensional magnetic field structure can provide a significant reference to experimental magnetic measurement.

Acknowledgments

The first author is grateful to Prof. Yu of the Max-Planck-Institut für Plasmaphysik for his instructive remarks and suggestions. Appreciation is also expressed to Prof. Zhuang, Prof. Chen, Dr. Ding, Dr. Wang, Dr. Xu, Dr. Jiang, and Dr. Wang for their encouragement and useful advice.

References

[1] Rogers B N, Denton R E, Drake J F and Shay M A 2001 *Phys. Rev. Lett.* **87** 195004
[2] Buratti P and Giovannozz E 2003 *30th EPS Conference on Contr. Fusion and Plasma Phys.*, 7–11 July 2003, St. Petersburg, Russia, ECA Vol. **27A**, O-1.2A
[3] Buratti P, Giovannozzi E and Tudisco O 2003 *Plasma Phys. Contr. Fusion* **45** L9
[4] Wolfe S M, Hutchinson I H, Granetz R S, Rice J, Hubbard A, Lynn A, Phillips P, Hender T C, Howell D F, La Haye R J and Scoville J T 2005 *Phys. Plasmas* **12** 056110

[5] Craven W A and Wootton A J 1998 *Nucl. Fusion* **38** 585
[6] Waelbroeck F L and Fitzpatrick R 1997 *Phys. Rev. Lett.* **78** 1703
[7] Scoville J T and La Haye R J 2003 *Nucl. Fusion* **43** 250
[8] Rao B, Ding Y H, Yu K X, Jin W, Hu Q M, Yi B, Nan J Y, Wang N C, Zhang M and Zhuang G 2013 *Rev. Sci. Instrum.* **84** 043504
[9] Yu Q, Günter S, Kikuchi Y and Finken K H 2008 *Nucl. Fusion* **48** 024007
[10] Cole A and Fitzpatrick R 2006 *Phys. Plasmas* **13** 032503
[11] Elgriw S, Liu D, Asai T, Hirose A and Xiao C 2011 *Nucl. Fusion* **51** 113008
[12] Yu Q, Günter S and Scott B D 2003 *Phys. Plasmas* **10** 797
[13] La Haye R J and Buttery R J 2009 *Phys. Plasmas* **16** 022107
[14] Riconda C, De Benedetti M and Ottaviani M 1999 *Phys. Plasmas* **6** 2762
[15] Hu Q M, Yu Q, Rao B, Ding Y H, Hu X W, Ge Z and the J-TEXT Team 2012 *Nucl. Fusion* **52** 083011
[16] Wesson J 2011 *Tokamaks* (4th Edn.) (New York: Oxford University Press) pp. 105–107
[17] Hu X W 2006 *Base of Plasma Theory* (Bejing: Peking University Press)
[18] Ding Y H, Zhuang G and Pan Y 2009 *Plasma Science and Technology* 11 456
[19] White R B 2001 *The Theory of Toloidally Confined Plasmas* (2nd Edn.) (Princeton: Princeton University Press)
[20] Freidberg J P 2007 *Plasma Physics and Fusion Energy* (Cambridge: Cambridge University Press)
[21] Liu M H 2013 16*nd National Conference on Plasma Science and Technology,* August 2013, Shanghai, China